Developmental Cell
Resource

A Genome-Wide siRNA Screen Reveals Multiple mTORC1 Independent Signaling Pathways Regulating Autophagy under Normal Nutritional Conditions

Marta M. Lipinski,[1] Greg Hoffman,[1,4] Aylwin Ng,[2,4] Wen Zhou,[1] Bénédicte F. Py,[1] Emily Hsu,[1] Xuxin Liu,[3] Jason Eisenberg,[2] Jun Liu,[3] John Blenis,[1] Ramnik J. Xavier,[2] and Junying Yuan[1,*]
[1]Department of Cell Biology, Harvard Medical School, 240 Longwood Avenue, Boston, MA 02115, USA
[2]Center for Computational and Integrative Biology, Massachusetts General Hospital, Harvard Medical School, 185 Cambridge Street, Boston, MA 02114, USA
[3]Department of Statistics, Harvard University, 1 Oxford Street, Cambridge, MA 02138, USA
[4]These authors contributed equally to this work
*Correspondence: junying_yuan@hms.harvard.edu
DOI 10.1016/j.devcel.2010.05.005

SUMMARY

Autophagy is a cellular catabolic mechanism that plays an essential function in protecting multicellular eukaryotes from neurodegeneration, cancer, and other diseases. However, we still know very little about mechanisms regulating autophagy under normal homeostatic conditions when nutrients are not limiting. In a genome-wide human siRNA screen, we demonstrate that under normal nutrient conditions upregulation of autophagy requires the type III PI3 kinase, but not inhibition of mTORC1, the essential negative regulator of starvation-induced autophagy. We show that a group of growth factors and cytokines inhibit the type III PI3 kinase through multiple pathways, including the MAPK-ERK1/2, Stat3, Akt/Foxo3, and CXCR4/GPCR, which are all known to positively regulate cell growth and proliferation. Our study suggests that the type III PI3 kinase integrates diverse signals to regulate cellular levels of autophagy, and that autophagy and cell proliferation may represent two alternative cell fates that are regulated in a mutually exclusive manner.

INTRODUCTION

Autophagy is an evolutionarily conserved catabolic process mediating turnover of intracellular constituents in a lysosome-dependent manner (Levine and Klionsky, 2004). In unicellular eukaryotes autophagy serves as a survival mechanism during periods of starvation by promoting intracellular recycling (Levine and Klionsky, 2004; Levine and Kroemer, 2008). In metazoa autophagy functions as an important intracellular catabolic mechanism involved in cellular homeostasis during development and adult life, by mediating the turnover of malfunctioning, aged, or damaged proteins and organelles (Levine and Kroemer, 2008). Autophagy can also be activated in response to many forms of cellular stress beyond nutrient starvation, including DNA damage, endoplasmic reticulum (ER) stress, reactive oxygen species, and on invasion by intracellular pathogens. On the organismal level, autophagy has been shown to participate in both innate and acquired immunity (Schmid and Munz, 2007), tumor suppression (Liang et al., 1999; Mathew et al., 2007a; Mathew et al., 2007b), and protection from neurodegeneration (Hara et al., 2006; Komatsu et al., 2006).

The signaling mechanisms leading to the activation of autophagy under nutrient starvation conditions have been extensively characterized. Inactivation of the mTORC1 kinase, a downstream effector of the type I PI3 kinase/Akt signaling, is critical for the activation of autophagy under these conditions (Levine and Klionsky, 2004; Levine and Kroemer, 2008). However, cells in complex multicellular eukaryotes such as mammals rarely experience nutrient deprivation under physiological conditions. Nevertheless, autophagy plays an essential role in maintenance of normal homeostasis at both cellular and organismal levels, as well as can be induced by a variety of cellular stresses under conditions when mTORC1 is known or expected to be active (Sakaki et al., 2008). Thus, there is an urgent need to understand the mechanisms that regulate autophagy under normal nutritional conditions.

To address this question and to understand the global regulation of mammalian autophagy, we carried out a genome-wide image-based siRNA screen for genes involved in the regulation of autophagy under normal nutrient conditions. Additionally we developed and executed a series of high-throughput characterization assays and screens allowing us to characterize the hit genes and further the understanding of the global regulation of mammalian autophagy. Our data indicate that under normal nutrition autophagy is regulated by a wide array of extracellular factors, including growth factors, cytokines, and chemokines. This response is mediated by a variety of cell surface receptor signaling pathways and, unlike during starvation, can be regulated in mTORC1 independent manner.

RESULTS

Genome-Wide siRNA Screen for Genes Regulating Autophagy

To identify new genes involved in the regulation of autophagy in mammals we screened a human genomic library containing

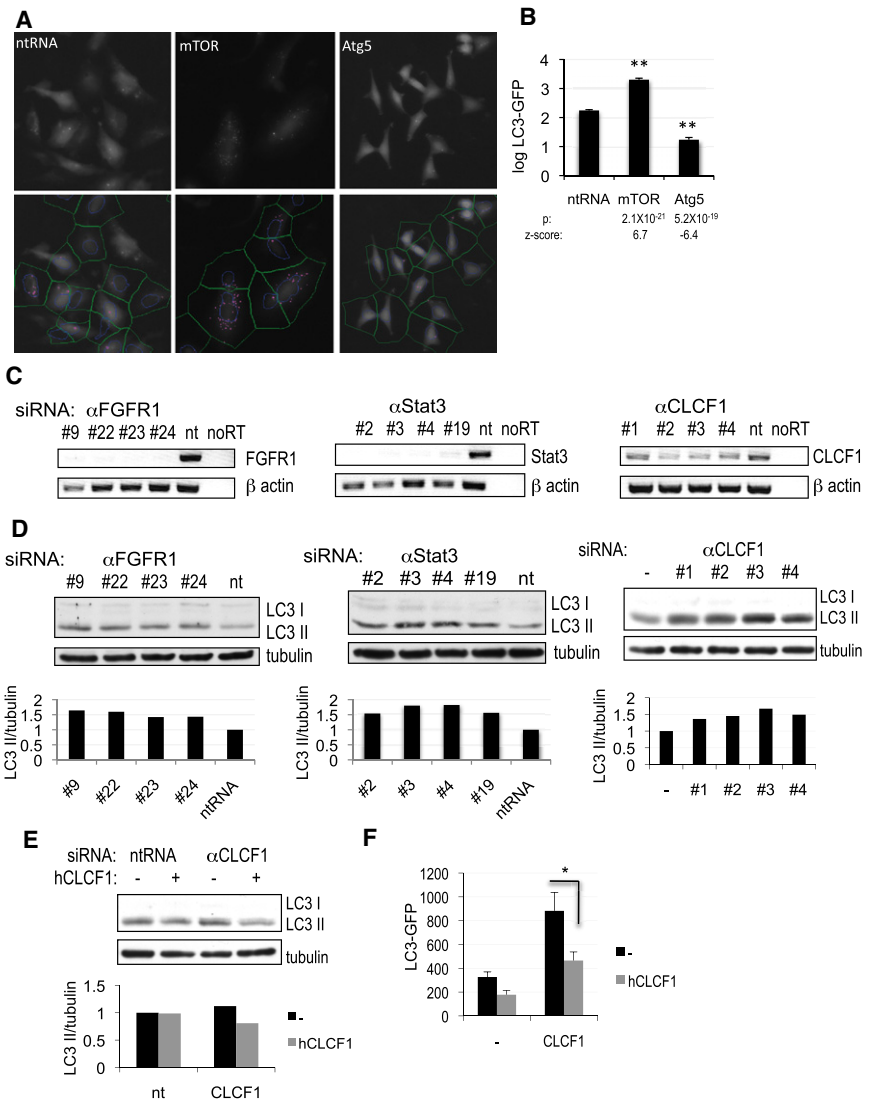

Figure 1. High-Throughput Image-Based Screen for Genes Regulating Autophagy

(A) H4 cells stably expressing LC3-GFP were transfected with nontargeting siRNA (ntRNA) or siRNA against mTOR or Atg5 for 72 hr, fixed, counterstained with Hoechst, and imaged on a high-throughput fluorescent microscope (10×). The bottom panels show results of image segmentation used for quantification of the ratio of soluble (diffuse cytosolic) versus autophagosome-associated (punctate) LC3-GFP: blue, nuclei; green, cell segmentation; pink, autophagosomal LC3-GFP.

(B) Quantification of data from (A).

(C) Confirmation of knockdown of selected screen hits by RT-PCR. H4 cells were transfected with indicated siRNAs for 72 hr.

(D) Confirmation of changes in levels of autophagy after knockdown of FGFR1, Stat3, or CLCF1 by western blot with antibodies against LC3. E64d (10 μg/mL) was added to the media for 8 hr before cells were harvested. Quantification of LC3 II/tubulin ratio is shown.

(E and F) Exogenous CLCF1 can suppress increase in autophagy induced by knockdown of CLCF1. H4 (E) or H4 LC3-GFP (F) cells were transfected with nontargeting siRNA (nt) or siRNA against CLCF1 and grown in the absence or presence of 100 ng/mL human CLCF1. Levels of autophagy were assessed by western blot (E) or by quantification of autophagosomal LC3-GFP (F). All error bars are SEM. *p = 0.05 based on two-tailed Student's t test (n ≥ 10).

siRNA pools targeting 21,121 genes, with four independent siRNA oligonucleotides for each gene. To quantify levels of autophagy, we used human neuroblastoma H4 cells stably expressing the LC3-GFP reporter (Shibata et al., 2006). In this system, transfection of siRNA targeting the essential autophagy mediator ATG5 led to significant downregulation of autophagy, as assessed by a reduction in the number and intensity of LC3-GFP positive autophagosomes (Figures 1A and 1B) as well as a decrease in endogenous LC3II levels on a western blot (see Figure S1A available online) (Klionsky et al., 2008). Conversely, transfection of siRNA targeting subunits of mTORC1, mTOR or Raptor, led to increased levels of autophagy (Figures 1A and 1B; Figures S1B and S1C). The primary screen resulted in the identification of 574 genes (2.7%) that knockdown led to a significant ($p < 0.02$) decrease or increase in LC3-GFP positive autophagosome formation. The candidate genes were then confirmed in a secondary screen in which the four pool siRNAs targeting different regions of the same gene, were evaluated separately. A total of 236 of the candidate genes (41%) were confirmed with at least two independent siRNA oligonucleotides resulting in significant increase or decrease in the levels of autophagy as compared to nontargeting siRNA controls (Figure 2A and Table 1; Table S1) ($p < 0.01$). The hit genes included 21 (9%) genes known to be involved or implicated in the regulation of autophagy, including ATG5, ATG7, IGF1, Rab7, and calpain-1 (Table S2). The ability to identify these known autophagy genes provides an important validation of our screening method.

As further validation of our hits, we confirmed knockdown of a selected group by RT-PCR and verified their ability to induce autophagy by western blot (Figures 1C and 1D). Importantly, stimulation of autophagy by knockdown of the cardiotrophin-like cytokine factor 1 (CLCF1), one of the cytokines identified in the screen, was suppressed in the presence of exogenous human CLCF1, demonstrating specificity of the observed phenotype (Figures 1E and 1F).

Although our screen was conducted under normal nutritional conditions when levels of autophagy are low, we were able to uncover a small set of hits (17. 7% of all confirmed genes) that resulted in the suppression of autophagy. Consistent with the function of these genes in mediation of autophagy, knockdown of a large fraction (35%) of these genes was able to downregulate autophagy in the presence of rapamycin, a potent mTORC1 inhibitor and well-known inducer of autophagy (Figure 2A; Table S3) (Klionsky et al., 2008; Levine and Kroemer, 2008).

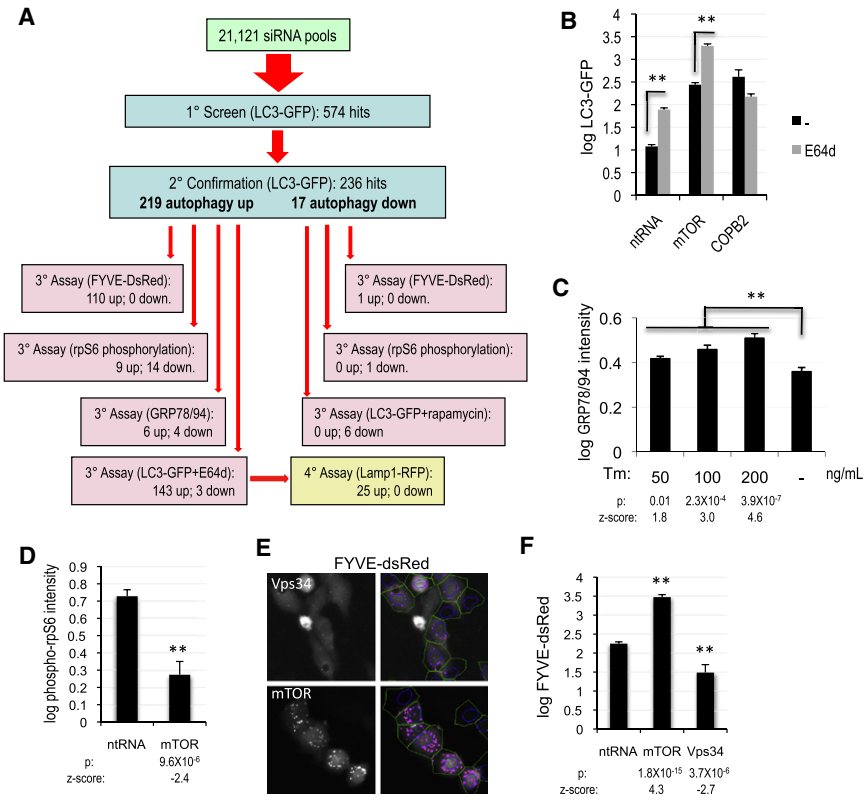

Figure 2. High-Throughput Characterization of the Autophagy Screen Hits

(A) Summary of all screen and characterization assays and their results.

(B) Quantification of levels of autophagy in H3 LC3-GFP cells transfected with nontargeting siRNA or siRNA against mTOR or COPB2. Lysosomal (10 μg/mL) protease inhibitor E64d was added for 8 hr before fixation. $p_{(mTOR)} = 6.5 \times 10^{-17}$.

(C) Quantification of ER stress in H4 cells treated with indicated levels of tumicamycin (Tm) for 24 hr by in-cell western assay with antibody against GRP78 and GRP94.

(D) Quantification of mTORC1 activity by in-cell western assay with antibody against phospho-rpS6 (Ser235/236) in H4 cells transfected with nontargeting siRNA or siRNA against mTOR for 72 hr.

(E) To assess the type III PI3 kinase activity, H4 cells stably expressing the PtdIns3P reporter FYVE-dsRed were transfected with siRNA against mTOR or Vps34. Right-hand panels represent the results of image segmentation used for quantification of the ratio of soluble (diffuse cytosolic) versus vesicle-associated (punctate) FYVE-dsRed: blue, nuclei; green, cell segmentation; pink, vesicular FYVE-dsRed.

(F) Quantification of data from (E). All error bars are SEM ($n \geq 6$).

High-Throughput Characterization of the Hit Genes

Because knockdown of the vast majority of hits (219, 93% of all confirmed) led to the induction of autophagy, our subsequent analyses concentrated on this group of genes. To elucidate the molecular pathways involved in regulation of autophagy by the candidate genes, we developed and carried out a series of additional high-throughput assays and screens to characterize the hits (Figure 2A). Accumulation of autophagosomal LC3-GFP can be due to either increased initiation of autophagy or to a block in degradation of autophagosomes. To distinguish between these possibilities, we evaluated induction of autophagy in the presence of the inhibitor of lysosomal proteases E64d. As expected, treatment with E64d led to a significant increase in levels of autophagy after knockdown of mTOR, but did not affect levels of autophagy induced by knockdown of the coatamer subunit COPB2, which is predicted to inhibit general vesicular trafficking (Figure 2B). Knockdown of 143 genes (69% of 206 tested) led to significantly higher induction of autophagy in the presence than in the absence of E64d (Table 1; Table S1), suggesting that similarly to starvation or inhibition of mTORC1, loss of these genes results in enhanced initiation of autophagy. On the other hand, the 63 (31%) genes that knockdown was unable to induce autophagy in the presence of E64d, likely cause the accumulation of autophagosomal LC3-GFP by blocking maturation and/or degradation of autophagosomes. For 24 of those genes, this may be due to a general defect in lysosomal proteolysis as induction of autophagy on loss of these genes was accompanied by significant expansion of the lysosomal compartment, as assessed by the accumulation of lysosomal reporter protein Lamp1-RFP (Figures S2A and S2B and Table S4).

Autophagy is often induced in response to various forms of cellular stress, including ER stress (Ogata et al., 2006; Yorimitsu et al., 2006). In our screen we observed that the accumulation of LC3-GFP was sometimes associated with decreased cell viability (Table S1), raising the question as to whether these cases may reflect a general response to cellular stress rather than a specific function in the regulation of autophagy. To assess that, we carried out an in-cell-western assay to measure the expression levels of GRP78 and GRP94, specific markers of ER stress. As expected, treatment with the inducer of ER stress, tunicamycin, led to a dose-dependent upregulation of GRP78 and GRP94 (Figure 2C), as well as an increase in autophagy (data not shown). However, with just a few exceptions (6 of 188 genes tested, 3%) (Table S5), we were unable to detect significant upregulation of ER stress after knockdown of the hit genes. Therefore, ER stress does not seem to be a major contributor to the induction of autophagy observed in our screen.

We evaluated the contribution of mTORC1, an essential suppressor of starvation-induced autophagy (Levine and Klionsky, 2004), by an in-cell-western assay of the phosphorylation status of a downstream target of mTORC1 signaling, the ribosomal protein S6 (rpS6) (Hoffman et al., 2010). As expected, transfection of siRNA against mTOR led to a significant decrease in the levels of rpS6 phosphorylation as compared to nontargeting siRNA (Figure 2D). Surprisingly, induction of autophagy was strongly correlated with downregulation of mTORC1 activity for only 14 (6%) of the 219 confirmed genes (Figure 2A; Table S1).

Table 1. Genes Regulating and Mediating Autophagy Identified in the Screen

Gene Symbol	Gene ID	Gene Symbol	Gene ID	Gene Symbol	Gene ID	Gene Symbol	Gene ID
Genes in which knockdown increases autophagy flux							
ADMR	11318	FANCC	2176	MMP17	4326	SCOTIN	51246
ADRA1A	148	FBXL20	84961	MUC3A	4584	SDHB	6390
AGER	177	FGFR1	2260	MYL3	4634	SEMA4B	10509
ARSE	415	FRAG1	27315	NAGK	55577	SETDB1	9869
ATG16L2	89849	GABBR2	9568	NCR3	259197	SF3A2	8175
AURKA	6790	GHSR	2693	NFIL3	4783	SIDT1	54847
BAI3	577	GJA4	2701	NNMT	4837	SIX2	10736
BAIAP2	10458	GNAI1	2770	NPTX1	4884	SLC25A19	60386
C18orf8	29919	GNG11	2791	NUDT1	4521	SMARCD1	6602
CAMKV	79012	GNG5	2787	OGDH	4967	SOD1	6647
CAPN1	823	GNRH2	2797	P2RX1	5023	SORCS2	57537
CARKL	23729	GPX2	2877	PA2G4	5036	SP140	11262
CASP1	834	GRK6	2870	PAK6	56924	STAT3	6774
CDCA8	55143	GTF2IRD2	84163	PAQR6	79957	TACR2	6865
CDK5RAP3	80279	GTPBP4	23560	PCGF1	84759	TGFBI	7045
CDKN2D	1032	HIST2H3C	126961	PDCD5	9141	THBS2	7058
CEND1	51286	HIVEP2	3097	PFDN2	5202	TINP1	10412
CENPJ	55835	HLA-DRB1	3123	PFKL	5211	TLR3	7098
CHAF1B	8208	HMGCL	3155	PHB2	11331	TMPRSS5	80975
CHID1	66005	HRC	3270	PIGY	84992	TNF	7124
CHRND	1144	HSFY2	159119	PLDN	26258	TNFRSF17	608
CLCF1	23529	ICT1	3396	PLXNA2	5362	TRIM69	140691
CNKSR2	22866	IGF1	3479	POLR3G	10622	TRNT1	51095
COL14A1	7373	IRAK3	11213	PPFIA4	8497	TRPA1	8989
COPE	11316	ITGAV	3685	PRAF2	11230	TSPAN4	7106
COX5A	9377	KIAA0133	9816	PRKAG3	53632	TUBGCP6	85378
CPNE6	9362	KIAA0196	9897	PRKCZ	5590	UBE1L2	55236
CXCL12	6387	KRT18	3875	PROSC	11212	UBE2D1	7321
CYP27A1	1593	LIF	3976	PSD	5662	UNC13B	10497
DBX1	120237	LOC285643	285643	PTGER2	5732	USP19	10869
DDX24	57062	LOC388959	388959	PTMA	5757	USP24	23358
EP300	2033	MAP3K7IP1	10454	PTPRH	5794	WASF1	8936
EPHA6	203806	MATN3	4148	PTPRU	10076	WFDC2	10406
EVL	51466	MCCC1	56922	RBBP8	5932	XPO1	7514
F12	2161	MMACHC	25974	RFX1	5989	ZFY	7544
FABP1	2168	MMP10	4319	SCAMP4	113178		
Genes in which knockdown increases autophagy due to decreased lysosomal processing							
ADM	133	DOCK8	81704	NTN2L	4917	SORBS3	10174
AMH	268	EGLN2	112398	NUPR1	26471	SSPN	8082
ARCN1	372	ERH	2079	NUTF2	10204	SUV39H1	6839
ASMT	438	FCER1A	2205	PLAGL2	5326	TAF2	6873
BGN	633	FXYD2	486	PLCH2	9651	TH	7054
C11orf68	83638	GJA3	2700	PNKD	25953	TNFRSF19L	84957
C2orf13	200558	HMBS	3145	PPARD	5467	TOM1	10043
C5AR1	728	HNRPK	3190	PRKAA2	5563	TRAF1	7185
CCT4	10575	HNRPM	4670	PRKCA	5578	TRHR	7201
CD300C	10871	HNRPU	3192	PTCRA	171558	TRIM8	81603
CD79A	973	HOXD11	3237	QSCN6	5768	TRIP6	7205
CENPE	1062	IHPK3	117283	RAB7A	7879	TUBB2A	7280

Table 1. *Continued*

Gene Symbol	Gene ID	Gene Symbol	Gene ID	Gene Symbol	Gene ID	Gene Symbol	Gene ID
CHKA	1119	INTS4	92105	RAGE	5891	USP54	159195
CKAP5	9793	MKLN1	4289	RANGAP1	5905	UTS2R	2837
CLCN1	1180	NAT9	26151	RELN	5649	ZBTB16	7704
COPB2	9276	NLK	51701	RORC	6097		
Genes in which knockdown increases autophagy (flux not determined)							
BPGM	669	KIF11	3832	NPTN	27020	TRPM3	80036
FGF2	2247	LOR	4014	RIPK1	8737		
GCM2	9247	OA48-18	10414	RNPEPL1	57140		
GFER	2671	NOXO1	124056	TACC2	10579		
Genes in which knockdown decreases autophagy							
ATG5	9474	KIF5C	3800	PDCL	5082	TCEB3	6924
ATG7	10533	LOC285647	285647	PGGT1B	5229	TPR	7175
CATSPER4	378807	MBP	4155	RELA	5970		
GAB1	2549	MEGF10	84466	SMYD3	64754		
GPR18	2841	NFKB1	4790	STIM1	6786		

Importantly, of the 143 genes, which similarly to starvation were able to enhance initiation of autophagy based on the E64d data, only 7 (5%) led to the suppression of mTORC1 activity, suggesting that only this small subset may be involved in the regulation of mTORC1. Conversely, knockdown of four of these genes (3%) led to both upregulation of autophagy and of mTORC1 activity (Table S1). Therefore, high mTORC1 activity may not be always incompatible with the induction of autophagy. The fact that knockdown of the vast majority of the screen hits did not affect mTORC1 activity suggests that these genes act either downstream or independently of this kinase. Because our hits include a large group of known upstream regulators of cellular signaling such as cytokines, growth factors, and their receptors (see Bioinformatics Analysis for details), our data implicate the existence of mTORC1 independent pathways regulating initiation of autophagy under normal nutritional conditions.

To characterize the contribution of the type III PI3 kinase, an important mediator of autophagy that regulation remains poorly understood (Levine and Klionsky, 2004), we used H4 cells stably expressing FYVE-dsRed reporter, which specifically binds to its product, PtdIns3P. Confirming the major role of the type III PI3 kinase in regulation of PtdIns3P levels in our system, transfection of siRNA against the catalytic component of this kinase, Vps34, led to a significant decline in FYVE-dsRed vesicle recruitment (Figures 2E and 2F). The relationship between mTORC1 and the type III PI3 kinase remains poorly understood. Although in some contexts Vps34 can play a positive role in the mediation of mTORC1 activation in response to amino acid stimulation (Byfield et al., 2005; Nobukuni et al., 2005), we did not observe significant downregulation of mTORC1 activity after knockdown of Vps34 (Figure S2C and S2D). On the other hand, Vps34 is known to function downstream of TORC1 during induction of autophagy in *Drosophila* (Juhasz et al., 2008), and inhibition of mTORC1 due to either starvation or rapamycin treatment of mammalian cells can lead to accumulation of vesicle associated PtdIns3P (Takahashi et al., 2007; Tassa et al., 2003; Zhang et al., 2007). Consistent with the data placing Vps34 downstream of mTORC1 in the regulation of autophagy, in our system knockdown of either mTOR or Raptor increased FYVE-dsRed vesicle recruitment (Figure 2E and 2F; Figure S2E). Using this system we determined that knockdown of 110 (47%) of the 236 confirmed genes led to a significant ($p < 0.05$) alteration in PtdIns3P levels, which correlated positively with the change in autophagosome formation (Table S1), suggesting that these genes act upstream of the type III PI3 kinase in the regulation of autophagy. These data confirm that the type III PI3 kinase plays an essential function in the regulation of autophagy under normal nutritional conditions and provide new insights into the mechanisms that regulate cellular levels of PtdIns3P.

Extracellular Factors Regulate Autophagy under Normal Nutrition

To gain further insight into the mechanisms by which the identified genes regulate cellular levels of autophagy, we used bioinformatics analysis. Molecular function analysis of the 236 confirmed hits using Gene Ontology (GO) showed a highly significant enrichment in kinases ($p = 0.0006$), proteins with receptor activity ($p = 7.7 \times 10^{-5}$) and extracellular matrix proteins ($p = 0.03$) (Figure 3A; Table S6). The latter categories suggest that extracellular environment including the presence of growth factors, hormones and cytokines, as well as extracellular matrix and cell-cell contacts, may play especially important function in the regulation of autophagy under normal nutritional conditions. The results of GO biological process analysis also showed significant enrichment in signaling molecules ($p = 2.8 \times 10^{-7}$) (Figure 3B; Table S7). In agreement with the function of extracellular clues in regulation of autophagy, further subdivision of these molecules revealed that the largest subgroup (49%) is involved in cell surface receptor signal transduction.

Cytokines Regulate Autophagy Independently of mTORC1

As an siRNA independent confirmation of the function of extracellular molecules in the regulation of autophagy, we treated

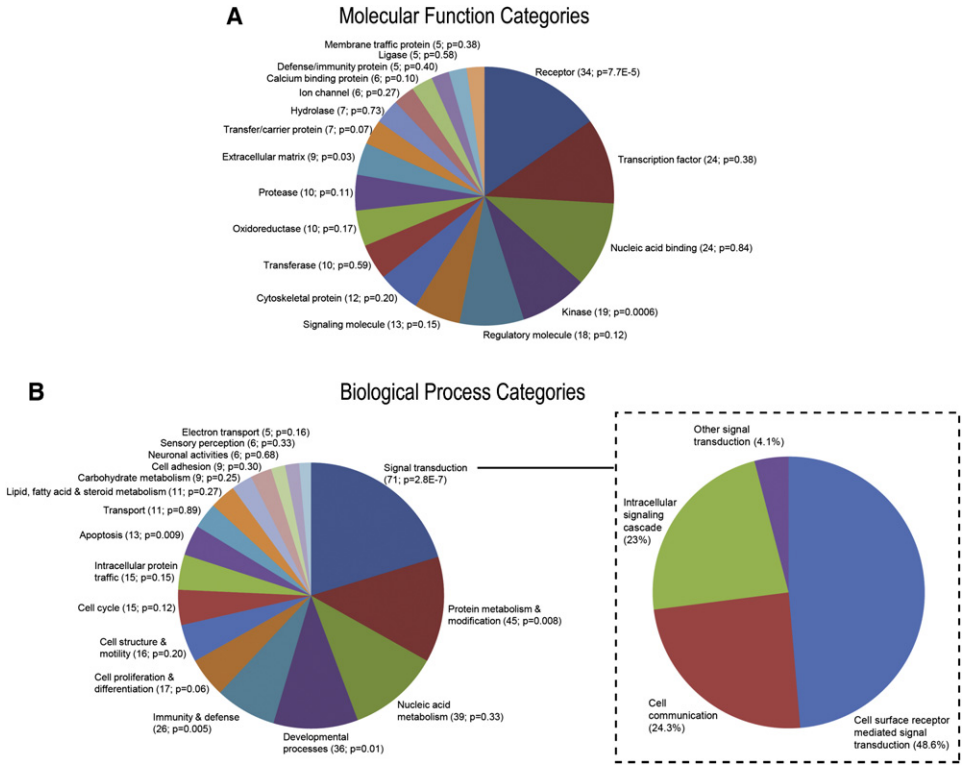

Figure 3. Autophagy Is Regulated in Response to Extracellular Stimuli through Multiple Receptor-Mediated Signaling Pathways

(A and B) Classification of the autophagy screen hits into molecular function (A) and biological process (B) categories according to the PANTHER system. In (B), subdivisions of the biological process "Signal Transduction" category are included. Categories with at least five genes are displayed. Categories with $p < 0.05$ (hypergeometric distribution) are considered enriched.

cells with several of the cytokines and growth factors identified as hits in our screen. Based on the results of the characterization assays, knockdown of IGF1, FGF2, LIF, CLCF1, and the chemokine SDF1 (CXCL12) resulted in mTORC1 independent increase in initiation of autophagy (Table S1). In agreement, treatment of H4 LC3-GFP cells grown in a serum-free medium with any of these cytokines led to a significant downregulation of autophagy as measured by LC3-GFP translocation (Figure 4A; Figure S3A). This data were furthermore confirmed in multiple cell lines (H4, HEK293, HeLa, and MCF7) by western blot (Figures 4B–4F; Figures S3B–S3L; data not shown). In agreement with the proposed function of cytokines in the regulation of autophagy, cells cultured in their absence displayed high basal levels of autophagy as assessed by accumulation of LC3II, which was suppressed partially by the addition of even single cytokines identified in the screen. Thus, we have identified a group of cytokines and growth factors that are both necessary and sufficient for the regulation of autophagy.

To determine whether downregulation of autophagy by these cytokines is due to reactivation of mTORC1 signaling, we inhibited mTORC1 by addition of rapamycin. As expected, treatment with rapamycin led to increases in the overall levels of autophagy (Figure 4). Despite efficient inhibition of mTORC1 as evidenced by dephosphorylation of both rpS6 and the S6 kinase, treatment with IGF1, FGF2, LIF, CLCF1, or SDF1 was able to reduce autophagy induced by rapamycin (Figures 4B–4F; Figure S4A). Similar results were obtained using an alternative mTORC1 inhibitor, Torin 1 (Figure S4B) (Thoreen et al., 2009). Additionally, siRNA mediated knockdown of mTOR also failed to prevent downregulation of autophagy by any of the cytokines (Figures S4C–S4H). Therefore, cytokines and growth factors identified in the screen are able to regulate autophagy via mTORC1 dependent as well as mTORC1 independent pathways. Additionally, only partial suppression of autophagy in the presence of rapamycin suggests that the effects of the Akt/mTORC1 and the cytokine-mediated mTORC1 independent pathways on the levels of autophagy may be additive, rather than mutually exclusive.

Growth-Promoting Pathways Negatively Regulate Autophagy

Bioinformatics analysis of the autophagy screen hits indicated significant enrichment for several canonical pathways known to mediate signaling from cell surface receptors (Figure 5A; Table S8). These pathways included the MAPK ($p = 0.039$), Stat3 ($p = 0.008$), and CXCR4 ($p = 1.1 \times 10^{-5}$) pathways regulated by the cytokines identified in the screen. FGF2 is known to activate the MAPK pathway. Indeed, we observed an increased level of phospho-ERK1/2 and phospho-RSK after treatment with FGF2 (Figure 5B). Confirming the essential function of the MAPK pathway, pretreatment with UO126, an inhibitor of MEK, attenuated inhibition of autophagy after addition of FGF2 (Figure 5B).

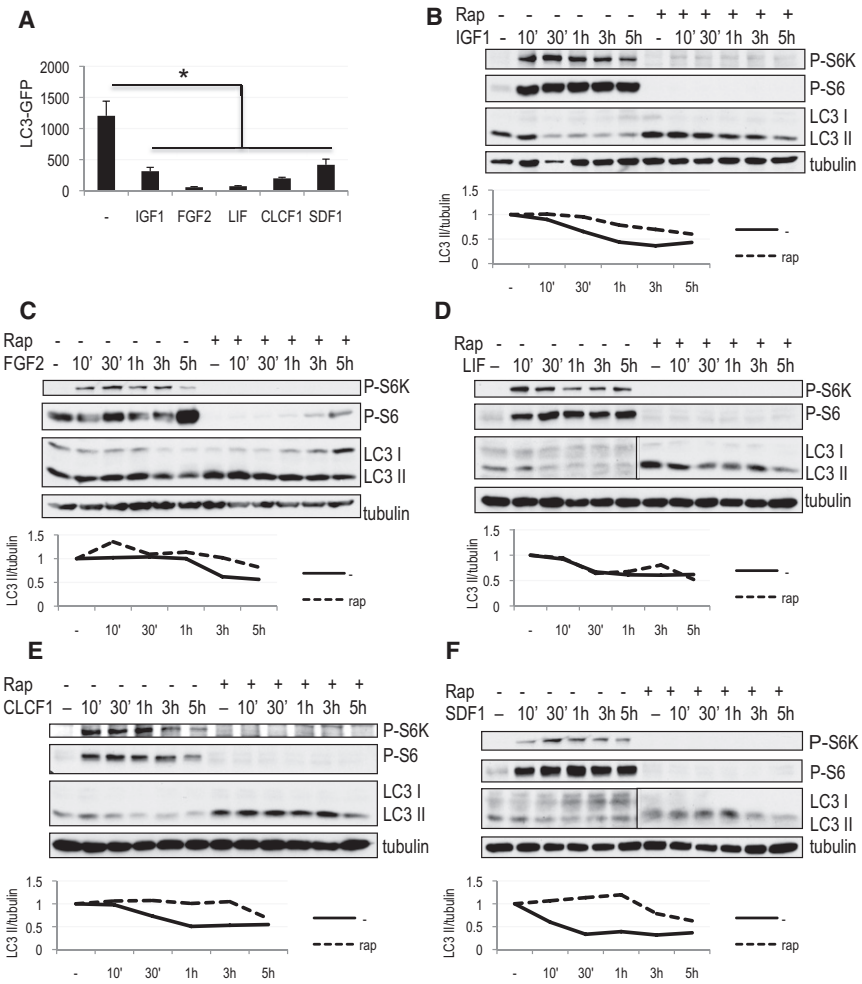

Figure 4. Cytokines Identified in the Screen Suppress Autophagy Independently of mTORC1 Activity

(A) Quantification of autophagy in H4 LC3-GFP cells grown in serum-free medium supplemented with indicated cytokines for 24 hr. All error bars are SEM. *$p < 0.05$ ($n \geq 8$).

(B–F) Cytokines are able to suppress autophagy in the absence and presence of rapamycin. H4 cells were grown in serum-free medium, followed by addition of 100 ng/mL IGF1 (B), 50 ng/mL FGF2 (C), 50 ng/mL LIF (D), 50 ng/mL CLCF1 (E), or 50 ng/mL SDF1 (F). Where indicated, cells were pretreated with 50 nM rapamycin 1 hr before the addition of cytokines. Levels of autophagy in the presence of 10 μg/mL E64d were assessed by western blot using antibody against LC3; mTORC1 activity was evaluated with antibodies against phospho-S6 (Ser235/236, P-S6) and phospho-S6 kinase (Thr389, P-S6K). Quantification of LC3 II/tubulin ratio is shown.

Interestingly, two of the genes identified in the screen, vinnexin (SORBS3) and tyrosine hydrolase (TH) (Table S1), are known ERK1/2 phosphorylation targets, suggesting that they may play a function in regulation of autophagy downstream of the MAPK pathway. Further confirming the important function of this pathway in the regulation of autophagy, we were able to construct a protein-protein interaction networks anchored by the hit genes belonging to the MAPK pathway (Figure 5C), which encompasses 42 (18%) of all the hit genes and directly connects to the known autophagy machinery through the interaction of the RIP kinase 1 (RIPK1) and PKCζ (PRKCZ) with p62/sequestrosome (SQSTM1). Additionally, analysis of the promoter regions of all the hit genes revealed significant enrichment in consensus sites for several transcription factors (Figure 5D), including three enriched sites for RSRFC4, a member of the serum response factor (SRF) family, and a known downstream target of MAPK signaling (Pollock and Treisman, 1991), suggesting additional involvement of transcriptional regulation by the MAPK pathway in control of autophagy under normal growth conditions.

Another hit gene pulled out of the screen as a negative regulator of autophagy was the transcription factor Stat3 (Table S1), a known mediator of LIF and CLCF1 signaling. Indeed, treatment with either LIF or CLCF1 increased activating phosphorylation of Stat3 (Figures 5E and 5F). Consistent with the essential function of Stat3, its siRNA mediated knockdown attenuated downregulation of autophagy in response to LIF (Figure 5F). Therefore, LIF and CLCF1 regulate autophagy through the Stat3 pathway. Analysis of the promoters of the core autophagy genes uncovered the presence of a consensus Stat3 site in the promoter of human Atg3 gene (V$STAT3_02, $p = 0.041$), raising the possibility that Stat3 may also contribute to the transcriptional regulation of the core autophagy machinery.

In addition to activating mTORC1, Akt is known to directly phosphorylate and inhibit Foxo3a, a transcription factor previously shown to positively regulate autophagy during muscle degeneration (Zhao et al., 2007). Indeed, phosphorylation of both Akt and Foxo3a was increased after IGF-1 treatment in both the absence and presence of rapamycin (Figure 5G; Figure S3B; data not shown). Inhibition of Akt by treatment with Akt inhibitor VIII attenuated phosphorylation of both Foxo3a and the mTORC1 target S6 kinase, as well as prevented inhibition of autophagy by IGF1 (Figure 5G). Therefore, under normal nutrient conditions IGF-1 regulates autophagy in a type I PI3 kinase/Akt dependent manner, likely through both the mTORC1 and Foxo3a pathways.

Cytokine Signaling Converges on the Type III PI3 Kinase

To further characterize the mechanism by which the cytokine dependent signaling pathways regulate autophagy, we treated FYVE-dsRed expressing H4 cells grown in serum-free media with IGF1, FGF2, LIF, CLCF1, or SDF1. All of the cytokines inhibited vesicular recruitment of FYVE-dsRed (Figure 6A; Figure S5A). Consistent with their ability to suppress autophagy in an mTORC1 independent manner, treatment with cytokines was able to suppress FYVE-dsRed in the presence of rapamycin

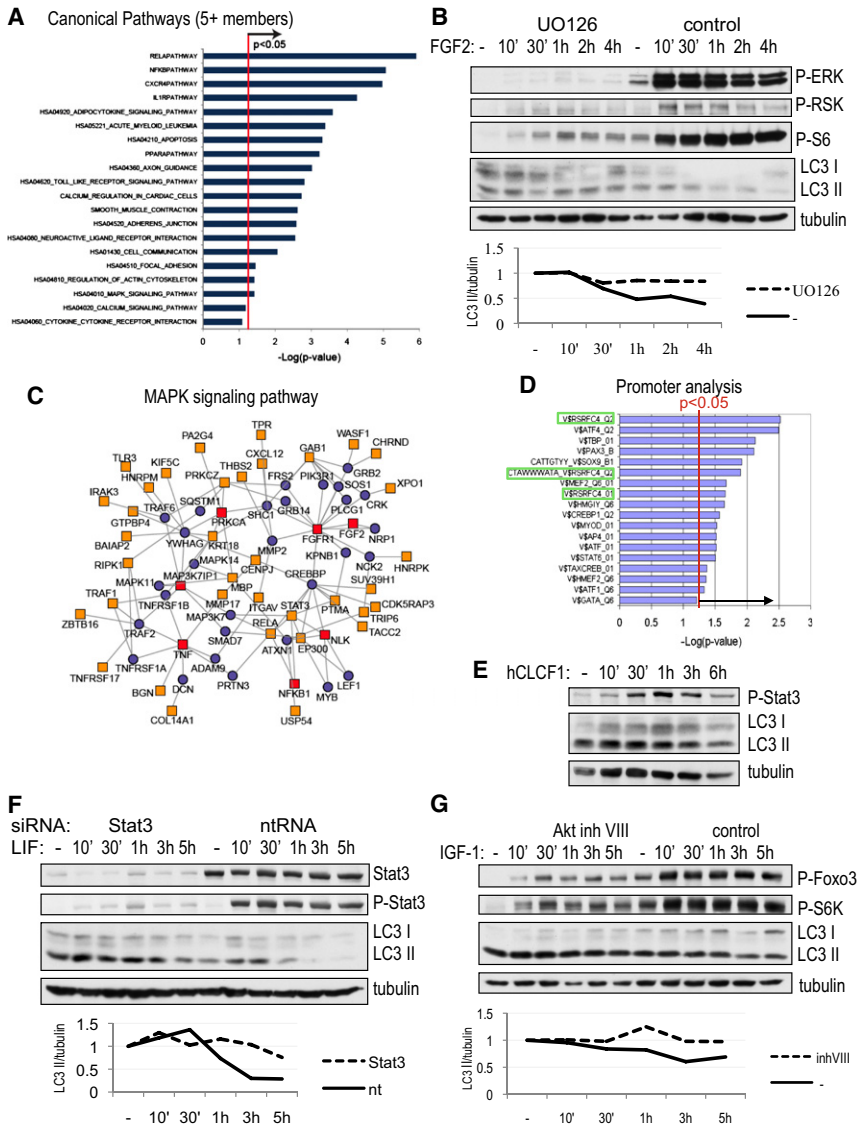

Figure 5. Growth Signaling Pathways Negatively Regulate Autophagy in Response to Cytokines

(A) Enrichment analysis of canonical pathways (MSigDB) among the hit genes relative to all genes examined in the screen. A p value <0.05 (hypergeometric distribution) is considered significant. Only categories with at least five genes are displayed.

(B) Downregulation of autophagy by 50 ng/mL FGF2 is prevented by addition of MEK inhibitor UO126. H4 cells were grown in serum-free media, levels of autophagy were assessed in the presence of 10 μg/mL E64d, with antibodies against LC3, inhibition MEK with phospho-ERK 1/2, phospho-RSK and phospho-S6 (Ser235/236). Quantification of LC3 II/tubulin ratio is shown.

(C) Network extensions of the canonical MAPK pathway. Using human interactome data, this pathway-centric network was constructed by anchoring on canonical pathway components and extended by establishing connections with other hit genes, including at most one intervening component. Red squares, screen hits that are part of the MAPK pathway; yellow squares, other screen hits; blue circles, intervening proteins.

(D) Enrichment analysis of *cis*-regulatory elements/transcription factor (TF)-binding sites in the promoters of the hit genes, using motif-based gene sets from MSigDB and TF-binding sites defined in the TRANSFAC database. SRF sites are highlighted.

(E) Phosphorylation of Stat3 after treatment with 50 ng/mL CLCF1.

(F) Downregulation of autophagy by 50 ng/mL LIF is prevented by siRNA mediated knockdown of Stat3. H4 cells were transfected with indicated siRNAs for 72 hr, than cells were treated as in (B). Protein levels and phosphorylation of Stat3 are shown.

(G) Suppression of autophagy by 100 ng/mL IGF1 is prevented by Akt inhibitor VIII. Cells were treated as in (B). Akt activity was assessed with antibodies against phospho-Foxo3a and phospho-rpS6.

(Figure 6B). This suggests that irrespective of the upstream signaling pathway, cytokines identified in the screen may regulate autophagy by modulating the levels of PtdIns3P. As treatment with 3MA, an inhibitor of the type III PI3 kinase, prevented further downregulation of PtdIns3P after treatment with cytokines (Figure 6C), this is dependent on the function of the type 3 PI3 kinase rather than other cellular sources of PtdIns3P. Confirming a crucial role of the type III PI3 kinase in regulation of autophagy downstream of cytokine signaling, treatment with any of the five cytokines was unable to further decrease levels of autophagy in H4 LC3-GFP cells deficient for Beclin 1 (Figure 6D; Figure S5B), the regulatory subunit of this kinase (Shibata et al., 2006).

In agreement with the cytokine data, knockdown of IGF1 or CLCF1 increased vesicular accumulation of FYVE-dsRed (Table S1). Additionally, we confirmed that inhibition of the Akt/TORC1, MAPK, and Stat3 pathways by knockdown of their components (mTOR, FGFR1, and Stat3/CLCF1, respectively) induced accumulation of PtdIns3P as assessed by increased levels of vesicular FYVE-dsRed (Figure 6E). Both, the accumulation of FYVE-dsRed and induction of autophagy by knockdown of mTOR, FGFR1, or CLCF1 was significantly attenuated after treatment with 3MA (Figures 6E and 6F) and in Beclin 1 and/or Vps34 knockdown cells (Figures S5C–S5E), confirming the critical involvement of the type III PI3 kinase in the regulation of autophagy downstream of the Akt/mTOR, MAPK, and Stat3 pathways.

DISCUSSION

We developed and executed what we believe to be an innovative high-throughput image-based screening and analysis approach, which allowed us to identify and characterize a group of 236 genes involved in the regulation of basal levels of autophagy under normal nutritional conditions. Further analysis showed that the screen hits are highly enriched for genes involved in receiving and mediating extracellular signaling. Our data show

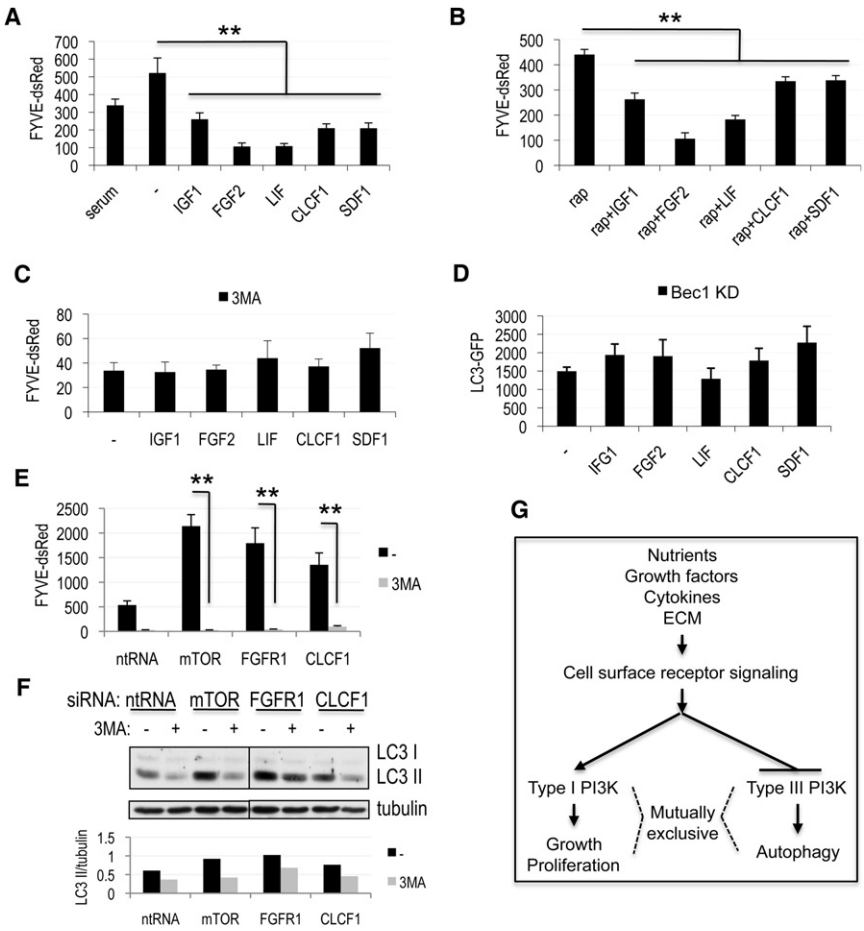

Figure 6. Regulation of Autophagy by Cytokines Is Dependent on the Type III PI3 Kinase

(A and B) Quantification of PtdIns3P levels in H4 FYVE-dsRed cells grown in serum-free medium supplemented for 24 hr with 100 ng/mL IGF1, 50 ng/mL FGF2, 50 ng/mL LIF, 50 ng/mL CLCF1, or 50 ng/mL SDF1, in the absence (A) or presence (B) of 50 nM rapamycin.

(C) Quantification of PtdIns3P levels in H4 FYVE-dsRed cells treated with indicated cytokines in the presence of the type III PI3 kinase inhibitor 3MA (10 mM).

(D) Quantification of levels of autophagy after cytokine treatment of Beclin 1 knockdown H4 LC3-GFP cells.

(E and F) Induction of PtdIns3P levels in H4 FYVE-dsRed cells (E) and upregulation of autophagy in H4 cells (F) after siRNA mediated knockdown of indicated genes is attenuated in the presence of 3MA. Cells were transfected with indicated siRNAs for 72 hr, 10 mM 3MA was added for 8 hr before cells were processed for analysis. For western blots 10 μg/mL E64d was added and quantification of LC3 II/tubulin ratio is shown. $^{**}p < 0.01$ ($n \geq 6$). All error bars are SEM.

(G) Model for opposing regulation of cell growth and autophagy by the type I and type III PI3 kinases in response to changes in extracellular environment.

that in higher eukaryotes, autophagy is regulated in a more versatile manner consistent with its expanded function in the maintenance of tissue and cell homeostasis and protection of organisms from cancer, neurodegeneration, and other diseases. The nutritional cues important for regulating autophagy in unicellular eukaryotes have been expanded to include an extensive array of environmental factors acting via multiple receptor-mediated signaling pathways, acting in an additive manner. Unlike starvation, the majority of these pathways are able to regulate autophagy in mTORC1 independent manner, instead converging on the type III PI3 kinase (see Graphical Abstract). Therefore, in addition to playing a necessary function during execution of autophagy, the type III PI3 kinase serves to integrate signals from many pathways to allow flexible adjustment of cellular levels of autophagy in response to diverse extracellular clues.

Interestingly, all of these pathways, including Akt/mTORC1, Akt/Foxo3, MAPK, Stat3, and CXCR4, in addition to negatively regulating autophagy as shown in this study, are well known to positively regulate cell growth and proliferation. Therefore, although autophagy is operating constantly at low levels under physiological conditions, induction of autophagy and cell growth may represent two alternative cell fates, which are regulated in a mutually exclusive manner (Figure 6G). This suggests that reducing levels of autophagy under normal nutritional condition may be advantageous in actively proliferating cells, including tumors. Conversely, high levels of autophagy may be incompatible with cell growth and proliferation, and their reduction could stimulate cell proliferation. Consistent with this hypothesis, mutations in at least six of the autophagy genes identified in the screen are causally implicated in human cancers and cancer syndromes (Table S9) (Futreal et al., 2004). We suggest that the mutually exclusive regulation of cell growth and autophagy is at least in part achieved through the differential activation of the type I PI3 kinase, which is known to suppress autophagy (Levine and Kroemer, 2008), and the type III PI3 kinase, in response to growth factors, cytokines, and other environmental cues. Thus, our study implicates the type III PI3 kinase as a tumor suppressor important for the negative control of cell growth and proliferation, providing a potential mechanism for increased rates of cancer incidence as a result of Beclin1 deficiency (Liang et al., 1999).

We believe our data provides important insights into the global regulation of autophagy, provides a rich resource, and points out novel avenues for further study of this essential cellular catabolic pathway. Our study highlights the use of combining multilevel screening, characterization, and bioinformatics analysis to elucidate global regulation of a complex biological process.

EXPERIMENTAL PROCEDURES

Cell Lines and Culture Conditions

H4 human neuroblastoma cells (Krex et al., 2001) were cultured under standard TC conditions in DMEM media supplemented with 10% normal calf

serum, 1× penicillin/streptomycin, and 1× Na pyruvate (Invitrogen). LC3-GFP, FYVE-dsRed, and LC3-GFP pSRP-Beclin1 knockdown H4 cells have been described previously (Shibata et al., 2006; Zhang et al., 2007). To create a stable line expressing Lamp1, H4 cells were transfected with Lamp1-RFP plasmid, followed by selection with 0.4 mg/mL G418.

For the cytokine assays cells were seeded at 0.5×10^5 in full medium. After 24 hr, cells were transferred to serum-free medium (DMEM or OptiMEM, Invitrogen); growth factors were added for 6–24 hr: human LIF (GenScript Corporation, 50 ng/mL), human FGF2 (ProSpec, 50 ng/mL), human IGF1 (ProSpec, 100–200 ng/mL), human CLCF1 (R&D Systems, 50 ng/mL), or human SDF1 (ProSpec, 50–100 ng/mL). Where indicated, rapamycin or Torin 1 (a gift from Dr. Nathaniel Gray, Harvard Medical School, Boston, MA) was added at the same time at 50 nM. For western assays, cells were cultured overnight in serum-free media, followed by addition of indicated cytokines and 10 μg/mL lysosomal protease inhibitor E64d (Sigma). For signaling pathway analysis cells were pretreated with indicated inhibitors for 1 hr before addition of cytokines and E64d, or transfected with indicated siRNAs at the time of initial plating. For CLCF1 complementation cells were transfected with indicated siRNAs and plated in full media supplemented with 100 ng/mL human CLCF1 and incubated for 72 hr. E64d was added for the last 6–8 hr before cell lysis.

siRNA Transfection

For the primary screen we used an arrayed library of 21,121 siRNA pools covering the vast majority of the human genome (Dharmacon si*ARRAY* siRNA library [Human Genome, G-005000-05], Thermo Fisher Scientific, Lafayette, CO). Each pool consisted of four oligonucleotides targeting a different region of the same gene. Each assay plate included the following controls: nontargeting siRNA, mTOR, ATG5, and PLK1 (transfection efficiency control) siRNA. siRNAs were transiently transfected in triplicate into H4 cells stably expressing LC3-GFP reporter at 40 nM final concentration using reverse transfection. HiPerfect reagent (QIAGEN) was diluted 1:20 in DMEM and 8 uL/well of the mixture was aliquoted into 384-well plates using WellMate liquid handling unit (Matrix). Two microliters of 1 uM-arrayed siRNA pools/well were added robotically using Velocity11 Bravo. After 30 min incubation, 500 cells/well in 40 uL full media were added using WellMate. Cells were incubated for 72 hr under standard culture conditions, counterstained with 0.5 μM Hoechst 33342 (Invitrogen) for 1 hr, and fixed with 30 uL of 8% paraformaldehyde for 30 min. Cells were washed three times with PBS using Velocity11 ELX405 Plate Washer (Bio-Tek).

For the secondary screen, we used a deconvolved library in which the four components of each siRNA pool were separated into individual wells. The cells were transfected and treated as for primary screen except that siRNAs were used at 30 nM final concentration and HiPerfect was diluted 1:30 in OptiMEM (Invitrogen). The secondary screen transfections were done in two rounds, for a total of five replica plates, using a 1:1 mixture of LC3-GFP and FYVE-dsRed or Lamp1-RFP cells. All tertiary characterization screens were carried out in either triplicate or duplicate. Each assay plate included 10–12 wells of nontargeting siRNA as well as mTOR, ATG5, PLK1, and/or Vps34 siRNA controls. To evaluate the contribution of inhibition of lysosomal degradation to the induction of autophagy, E64d was added at 10 μg/mL where indicated for the last 8 hr before fixation.

For follow-up assays, cells were transfected in 96-, 24-, or 6-well plates using reverse transfection with 1–6 μl HiPerfect/mL, 10–30 nM final siRNA concentration, and cells at 5×10^4 to 2×10^5 cells/mL, depending on the cell type. Cells were harvested 48–72 hr after transfection.

Imaging and Image Quantification

Cells were imaged on an automated CellWoRx microscope (Applied Precision) at 10× magnification and 350 nm (Hoechst), 488 nm (LC3-GFP), and 550 nm (Lamp1-RFP and FYVE-dsRed) wavelengths. All images were quantified using VHSscan and VHSview image analysis software (Cellomics). Total cell number, total LC3-GFP intensity/cell as well as number, area, and intensity of LC3-GFP positive autophagosomes/cell were scored. Dead and mitotic cells were excluded from analysis based on nuclear intensity. The final autophagy score for every well was obtained by multiplying total autophagosome intensity/cell times number of autophagosomes/cell and dividing by average cells intensity. This formula was empirically determined to most accurately measure LC3-GFP translocation from cytosol into autophagosomes as reflected by consistently significant *Z*-scores and p values when using siRNAs against mTOR and Atg5 controls under the assay conditions and to give the highest *Z*′-score (0.52, where $Z' = 1 - (3SD_{mTOR} + 3SD_{Atg5})/(Ave_{mTOR} - Ave_{Atg5})$ (Zhang et al., 1999). FYVE-dsRed and Lamp1-RFP scores were obtained in a similar manner, except that in the case of Lamp1-RFP, which measures total accumulation of the reporter rather than its translocation, division by the average cell intensity was omitted.

In-Cell Western Assay

H4 cells were cultured in 384-well plates, fixed, and counterstained as described for the LC3-GFP assay. After imaging, the cells were permeabilized in PBS + 0.2% Tx-100 (PBST) and stained with Alexa-680 NHS-ester at 20 ng/mL for 15 min. Cells were washed with PBST and incubated for 30 min in blocking buffer (1:1 LiCOR blocking buffer/PBST) and overnight in rabbit-anti-rpS6 phospho-235/236 (Cell Signaling Technologies) or mouse-anti-KDEL (Stressgen) antibody at 1:1000 in blocking buffer. Cells were washed in PBST and stained with an IRDye-800-conjugated secondary antibody (LiCOR) at 1:1000. The plates were scanned on the Aerius infrared imaging system (LiCOR). The intensity of both, the rpS6 phospho-235/236 or KDEL staining, and of NHS-ester staining were integrated, and the normalized phospho-S6 or KDEL score was calculated for each well by dividing phospho-rpS6 or KDEL intensity by NHS-ester intensity (Hoffman et al., 2010).

Statistical Analysis

All screen data were normalized by conversion to logarithmic scale. For primary screen, *Z*-scores were calculated based on plate median (controls excluded) and median absolute deviation, with *Z*-score = (cell score − median plate score)/(plate median absolute deviation × 1.4826) (Chung et al., 2008). The screen hits were selected based on the median *Z*-score of the three replica-plates with cut-offs set at *Z*-score >1.7 or <−1.9 ($p < 0.02$). The same method was used for the rpS6 and KDEL secondary screens except the assays were carried out in duplicate. For LC3-GFP, FYVE-dsRed, and Lamp1-RFP secondary screens *Z*-scores were calculated based on nontargeting siRNA control ($n = 10$–12) mean and standard deviation (SD). For confirmation of hits in the LC3-GFP assay we required that at least two of four individual siRNA oligonucleotides for each gene had median *Z*-scores >1.5 or <−1.5 based on five replica plates and were consistent with the primary screen *Z*-score ($p < 0.01$). In all other secondary assays *Z*-scores >1.5 and <−1.5 were also considered significant. The final *Z*-scores for confirmed genes were calculated based on average *Z*-scores of all wells for oligonucleotides positive in the secondary LC3-GFP assay.

The correlation analysis between LC3-GFP and other secondary assays was carried out based on individual assay well quadrant analysis: for each well a score of +1 was assigned if *Z*-scores for both features were >1.5 or <−1.5; a score of −1 if one *Z*-score was >1.5 while the other was <−1.5; a score of 0 if either *Z*-score failed to reach the cut-off. The individual well scores were than summed up for each gene for all oligonucleotides considered significant in the LC3-GFP secondary assay and divided by the total number of wells assayed for these oligonucleotides. A correlation between features was considered to be positive if the final score was ≥ 0.5, negative if it was ≤ -0.5.

A double criteria was used for the identification of genes in which knockdown was able to induce autophagy in the presence of E64d: (1) knockdown of the gene in the presence of E64d was able to induce autophagy above the levels observed with nontargeting siRNA + E64d by at least 1.5 SD, and (2) treatment with E64d was able to increase levels of autophagy after knockdown of the gene by at least 1.5 SD.

Relative viability was calculated by dividing number of cells in each well based on Hoechst imaging by the average cell number in the plate. The reported viability for each hit gene reflects average viability of all wells for oligonucleotides positive in the secondary LC3-GFP assay.

Unless otherwise indicated, all remaining p values were calculated from a two-tailed Student's t test with equal variance. All error bars are standard error.

Western Analysis

Cells were lysed in Laemmli sample buffer, resolved on 12% SDS-PAGE, and transferred to PVDF membrane following standard protocols. The following

antibodies were used: phospho-Foxo3a and Atg5 (Sigma) at 1:500; LC3 (Novus), p62 (Pharmigen), phospho-S6K (Thr389), phospho-Akt (Ser473), Stat3, phospho-Stat3 (Tyr705), and mTOR (all from Cell Signaling) at 1:1000; phospho-S6 (Ser235/236) (Cell Signaling) and phospho-ERK 1/2 (Sigma) at 1:2000; tubulin (Sigma) at 1:5000. Blots were quantified using NIH ImageJ64 software.

Semiquantitative RT-PCR

Total RNA was prepared using RNeasy mini kit (QIAGEN). RNA (1.25 μg) was used for cDNA synthesis using SuperScript First-Strand Synthesis System for RT-PCR (Invitrogen) with oligo dT primers. Following primers were used: FGFR1 CTCCGGCCTCTATGCTTGCGTAAC and TGCGGCTGCGGGTCACT GTA, Stat3 ACCCCGGCTTGGCGCTGTCTCT and ACGGCTGCTGTGGGGT GGTTGG, CLCF1 TGGGCCTGGCGGATGGGATTATTA and TGGGTCAGCC GCAGTTTGTCATTG, β actin GACCTGACAGACTACCTCAT and AGACAGC ACTGTGTTGGCTA.

Bioinformatics Analysis

For enrichment analyses, genes were classified into functional categories including: biological process, molecular function (PANTHER classification system [Mi et al., 2005]), canonical pathways (MSigDB [Subramanian et al., 2005]), and transcription factor binding sites (MSigDB and TRANSFAC v7.4 (www.gene-regulation.com)). Genes for which no annotations could be assigned were excluded. To assess the statistical enrichment of these categories for the hit genes relative to their representation in the global set of genes examined, p values were computed using the hypergeometric probability distribution. Categories with $p < 0.05$ were considered enriched. Similar enrichment results were obtained independently of the details of the hit selection protocol.

Protein Interaction Network

The network was constructed by iteratively connecting interacting proteins, with data extracted from genome-wide interactome screens (Ho et al., 2002; Ito et al., 2001), databases: HPRD (Mishra et al., 2006), MINT (Chatr-aryamontri et al., 2007), REACTOME (Joshi-Tope et al., 2005), and curated literature entries implemented in the Perl programming language. The network is a graphical representation of protein-protein relationships, with components (gene products) represented as nodes and relationships (interactions) between components as edges.

SUPPLEMENTAL INFORMATION

Supplemental Information includes five figures and nine tables and can be found with this article online at doi:10.1016/j.devcel.2010.05.005.

ACKNOWLEDGMENTS

We thank N. Mizushima and N. Gray for reagents, C. Yi for critical reading of the manuscript, and the members of the Yuan lab and the ICCB-Longwood for help during this work. This work was supported in part by NIH grants R37 AG012859 and PO1 AG027916 to J.Y., AI062773 and DK043351 to R.J.X., R01 GM051405 and R21 NS059428 to J.B., and NSF grant DMS-0706989 to J.L. G.H. is supported by fellowships from the Helen Hay Whitney Foundation and the LAM Foundation, A.N. by the Crohn's and Colitis Foundation of America, and J.E. by CCIB Development Fund.

Received: October 24, 2009
Revised: February 11, 2010
Accepted: March 23, 2010
Published: June 14, 2010

REFERENCES

Byfield, M.P., Murray, J.T., and Backer, J.M. (2005). hVps34 is a nutrient-regulated lipid kinase required for activation of p70 S6 kinase. J. Biol. Chem. *280*, 33076–33082.

Chatr-aryamontri, A., Ceol, A., Palazzi, L.M., Nardelli, G., Schneider, M.V., Castagnoli, L., and Cesareni, G. (2007). MINT: the Molecular INTeraction database. Nucleic Acids Res. *35*, D572–D574.

Chung, N., Zhang, X.D., Kreamer, A., Locco, L., Kuan, P.F., Bartz, S., Linsley, P.S., Ferrer, M., and Strulovici, B. (2008). Median absolute deviation to improve hit selection for genome-scale RNAi screens. J. Biomol. Screen. *13*, 149–158.

Futreal, P.A., Coin, L., Marshall, M., Down, T., Hubbard, T., Wooster, R., Rahman, N., and Stratton, M.R. (2004). A census of human cancer genes. Nat. Rev. Cancer *4*, 177–183.

Hara, T., Nakamura, K., Matsui, M., Yamamoto, A., Nakahara, Y., Suzuki-Migishima, R., Yokoyama, M., Mishima, K., Saito, I., Okano, H., et al. (2006). Suppression of basal autophagy in neural cells causes neurodegenerative disease in mice. Nature *441*, 885–889.

Ho, Y., Gruhler, A., Heilbut, A., Bader, G.D., Moore, L., Adams, S.L., Millar, A., Taylor, P., Bennett, K., Boutilier, K., et al. (2002). Systematic identification of protein complexes in Saccharomyces cerevisiae by mass spectrometry. Nature *415*, 180–183.

Hoffman, G.R., Moerke, N.J., Hsia, M., Shamu, C.E., and Blenis, J.A. (2010). High-throughput, cell-based screening method for siRNA and small molecule inhibitors of mTORC1 signaling using the in cell Western technique. Assay Drug Dev. Technol. *8*, 186–199.

Ito, T., Chiba, T., Ozawa, R., Yoshida, M., Hattori, M., and Sakaki, Y. (2001). A comprehensive two-hybrid analysis to explore the yeast protein interactome. Proc. Natl. Acad. Sci. USA *98*, 4569–4574.

Joshi-Tope, G., Gillespie, M., Vastrik, I., D'Eustachio, P., Schmidt, E., de Bono, B., Jassal, B., Gopinath, G.R., Wu, G.R., Matthews, L., et al. (2005). Reactome: a knowledge base of biological pathways. Nucleic Acids Res. *33*, D428–D432.

Juhasz, G., Hill, J.H., Yan, Y., Sass, M., Baehrecke, E.H., Backer, J.M., and Neufeld, T.P. (2008). The class III PI(3)K Vps34 promotes autophagy and endocytosis but not TOR signaling in Drosophila. J. Cell Biol. *181*, 655–666.

Klionsky, D.J., Abeliovich, H., Agostinis, P., Agrawal, D.K., Aliev, G., Askew, D.S., Baba, M., Baehrecke, E.H., Bahr, B.A., Ballabio, A., et al. (2008). Guidelines for the use and interpretation of assays for monitoring autophagy in higher eukaryotes. Autophagy *4*, 151–175.

Komatsu, M., Waguri, S., Chiba, T., Murata, S., Iwata, J., Tanida, I., Ueno, T., Koike, M., Uchiyama, Y., Kominami, E., et al. (2006). Loss of autophagy in the central nervous system causes neurodegeneration in mice. Nature *441*, 880–884.

Krex, D., Mohr, B., Hauses, M., Ehninger, G., Schackert, H.K., and Schackert, G. (2001). Identification of uncommon chromosomal aberrations in the neuroglioma cell line H4 by spectral karyotyping. J. Neurooncol. *52*, 119–128.

Levine, B., and Klionsky, D.J. (2004). Development by self-digestion: molecular mechanisms and biological functions of autophagy. Dev. Cell *6*, 463–477.

Levine, B., and Kroemer, G. (2008). Autophagy in the pathogenesis of disease. Cell *132*, 27–42.

Liang, X.H., Jackson, S., Seaman, M., Brown, K., Kempkes, B., Hibshoosh, H., and Levine, B. (1999). Induction of autophagy and inhibition of tumorigenesis by beclin 1. Nature *402*, 672–676.

Mathew, R., Karantza-Wadsworth, V., and White, E. (2007a). Role of autophagy in cancer. Nat. Rev. Cancer *7*, 961–967.

Mathew, R., Kongara, S., Beaudoin, B., Karp, C.M., Bray, K., Degenhardt, K., Chen, G., Jin, S., and White, E. (2007b). Autophagy suppresses tumor progression by limiting chromosomal instability. Genes Dev. *21*, 1367–1381.

Mi, H., Lazareva-Ulitsky, B., Loo, R., Kejariwal, A., Vandergriff, J., Rabkin, S., Guo, N., Muruganujan, A., Doremieux, O., Campbell, M.J., et al. (2005). The PANTHER database of protein families, subfamilies, functions and pathways. Nucleic Acids Res. *33*, D284–D288.

Mishra, G.R., Suresh, M., Kumaran, K., Kannabiran, N., Suresh, S., Bala, P., Shivakumar, K., Anuradha, N., Reddy, R., Raghavan, T.M., et al. (2006). Human protein reference database–2006 update. Nucleic Acids Res. *34*, D411–D414.

Nobukuni, T., Joaquin, M., Roccio, M., Dann, S.G., Kim, S.Y., Gulati, P., Byfield, M.P., Backer, J.M., Natt, F., Bos, J.L., et al. (2005). Amino acids

mediate mTOR/raptor signaling through activation of class 3 phosphatidylinositol 3OH-kinase. Proc. Natl. Acad. Sci. USA *102*, 14238–14243.

Ogata, M., Hino, S., Saito, A., Morikawa, K., Kondo, S., Kanemoto, S., Murakami, T., Taniguchi, M., Tanii, I., Yoshinaga, K., et al. (2006). Autophagy is activated for cell survival after endoplasmic reticulum stress. Mol. Cell. Biol. *26*, 9220–9231.

Pollock, R., and Treisman, R. (1991). Human SRF-related proteins: DNA-binding properties and potential regulatory targets. Genes Dev. *5*, 2327–2341.

Sakaki, K., Wu, J., and Kaufman, R.J. (2008). Protein kinase Ctheta is required for autophagy in response to stress in the endoplasmic reticulum. J. Biol. Chem. *283*, 15370–15380.

Schmid, D., and Munz, C. (2007). Innate and adaptive immunity through autophagy. Immunity *27*, 11–21.

Shibata, M., Lu, T., Furuya, T., Degterev, A., Mizushima, N., Yoshimori, T., MacDonald, M., Yankner, B., and Yuan, J. (2006). Regulation of intracellular accumulation of mutant Huntingtin by Beclin 1. J. Biol. Chem. *281*, 14474–14485.

Subramanian, A., Tamayo, P., Mootha, V.K., Mukherjee, S., Ebert, B.L., Gillette, M.A., Paulovich, A., Pomeroy, S.L., Golub, T.R., Lander, E.S., et al. (2005). Gene set enrichment analysis: a knowledge-based approach for interpreting genome-wide expression profiles. Proc. Natl. Acad. Sci. USA *102*, 15545–15550.

Takahashi, Y., Coppola, D., Matsushita, N., Cualing, H.D., Sun, M., Sato, Y., Liang, C., Jung, J.U., Cheng, J.Q., Mule, J.J., et al. (2007). Bif-1 interacts with Beclin 1 through UVRAG and regulates autophagy and tumorigenesis. Nat. Cell Biol. *9*, 1142–1151.

Tassa, A., Roux, M.P., Attaix, D., and Bechet, D.M. (2003). Class III phosphoinositide 3-kinase–Beclin1 complex mediates the amino acid-dependent regulation of autophagy in C2C12 myotubes. Biochem. J. *376*, 577–586.

Thoreen, C.C., Kang, S.A., Chang, J.W., Liu, Q., Zhang, J., Gao, Y., Reichling, L.J., Sim, T., Sabatini, D.M., and Gray, N.S. (2009). An ATP-competitive mammalian target of rapamycin inhibitor reveals rapamycin-resistant functions of mTORC1. J. Biol. Chem. *284*, 8023–8032.

Yorimitsu, T., Nair, U., Yang, Z., and Klionsky, D.J. (2006). Endoplasmic reticulum stress triggers autophagy. J. Biol. Chem. *281*, 30299–30304.

Zhang, J.H., Chung, T.D., and Oldenburg, K.R. (1999). A Simple Statistical Parameter for Use in Evaluation and Validation of High Throughput Screening Assays. J. Biomol. Screen. *4*, 67–73.

Zhang, L., Yu, J., Pan, H., Hu, P., Hao, Y., Cai, W., Zhu, H., Yu, A.D., Xie, X., Ma, D., et al. (2007). Small molecule regulators of autophagy identified by an image-based high-throughput screen. Proc. Natl. Acad. Sci. USA *104*, 19023–19028.

Zhao, J., Brault, J.J., Schild, A., Cao, P., Sandri, M., Schiaffino, S., Lecker, S.H., and Goldberg, A.L. (2007). FoxO3 coordinately activates protein degradation by the autophagic/lysosomal and proteasomal pathways in atrophying muscle cells. Cell Metab. *6*, 472–483.